

HUBBLE SPACE TELESCOPE NICMOS IMAGING OF W3 IRS 5: A TRAPEZIUM IN THE MAKING?

S. T. MEGEATH¹, T. L. WILSON^{2,3}, M. R. CORBIN⁴

Draft version May 16, 2019

ABSTRACT

We present *Hubble Space Telescope* NICMOS imaging of W3 IRS 5, a binary high-mass protostar. In addition to the two protostars, NICMOS images taken in the F222M and F160W filters show three new 2.22 μm sources with very red colors; these sources fall within a region 5600 AU in diameter, and are coincident with a $\sim 100 M_{\odot}$, dense molecular clump. Two additional point sources are found within 0.4'' (800 AU) of one of the high-mass protostars; these may be stellar companions or unresolved emission knots from an outflow. We propose that these sources constitute a nascent Trapezium system in the center of the W3 IRS 5 cluster containing as many as five proto-OB stars. This would be the first identification of a Trapezium still deeply embedded in its natal gas.

Subject headings: ISM:individual(W3 IRS 5) — infrared:stars — stars: formation

1. INTRODUCTION

In the pursuit of obtaining a comprehensive understanding of star formation in our Galaxy, the formation of stars with masses greater than $10 M_{\odot}$ remains a challenging problem. It has become well established that massive stars form not in isolation, but in close proximity to other stars spanning the entire range of the initial mass function. Observationally, the gregarious nature of massive star formation has been established on three hierarchical levels. On the largest spatial scales, young massive stars are almost always found in clusters, with sizes around 0.5 pc (Hodapp 1994, Sollins & Megeath 2004). The more relevant scale for the formation of high-mass stars is that of a few thousand AU. On these spatial scales, massive stars are often found to be part of multiple systems and Trapezia. Trapezia, defined as non-hierarchical (and consequently, unstable) multiple systems, are commonly found within OB-associations and open clusters (Ambartsumian 1954, Sharpless 1954). Multiplicity around high-mass stars continues to even smaller separations; spectroscopic observations of massive stars show companions with separations of 10 AU or less (Mermilliod & Garcia 2001).

It is not clear whether OB stars form in these multiple systems, or whether the multiple systems are formed from subsequent dynamical interactions in the dense centers of young stellar clusters (Bonnell & Davies 1998, Kroupa, Aaserth & Hurley 2001). To date, the known examples of OB stars in multiple systems have already cleared their natal gas. If OB stars form with companions at separations ranging from a few AU to 1000 AU, then these companions may play an important role in mediating accretion onto OB stars by modifying accretion disks and envelopes, by adding extra mass to the system (Keto 2003), or through mergers (Bonnell & Bate 2002).

For this reason, it is essential to search for com-

panions of forming massive stars at the highest available angular resolution. A rare example of a binary high-mass protostar is W3 IRS 5, at a distance of 1.8 kpc (Imai et al. 2000). This infrared source was first resolved into a double infrared source by Howell, McCarthy & Low (1981) and Neugebauer, Becklin & Matthews (1982). The total luminosity is $2 \times 10^5 L_{\odot}$ (Campbell et al. 1995). Radio observations with the Very Large Array by Wilson et al. (2003) and van der Tak, Dianchi, & Tuthill (2005) show that each component of the infrared source is coincident with a radio continuum source with sizes < 240 AU. These *hypercompact* HII regions are perhaps the youngest detectable stage of a massive star. The W3 IRS 5 region is also the source of at least two outflows (Imai et al. 2000, Wilson et al. 2003). Megeath et al. (1996) found that the W3 IRS 5 cluster is in the center of an embedded cluster of 80-240 low mass stars. We report here HST NICMOS observations of W3 IRS 5 with an angular resolution of 350 AU.

2. OBSERVATIONS & DATA REDUCTION

The observations were taken in Cycle 7 using camera 2 of NICMOS onboard the *Hubble Space Telescope* (Thompson et al. 1998). A 3×3 map was made using a spiral-dither pattern with two dithers at each map position. The multiaccum mode was used with a total integration time of 128 sec for each image. The images were taken in the F110W, F160W and F222M filters. The data were reduced with the standard STSCI pipeline. The frames were then registered and mosaiced using a custom program written in the Interactive Data Language (IDL).

Photometry was obtained through a combination of aperture photometry and point spread function (PSF) fitting. The PSF was generated with the TinyTim program (Krist & Hook 1997). Using a custom IDL program, we fit the PSF to five point sources in the F222M mosaic: NIR1, NIR2, NIR2a, NIR2b and NIR4 (see Table 1). For NIR2, NIR2a and NIR2b, which are separated by less than 0.4'', we fit three PSFs simultaneously. We also fit PSFs to five isolated point sources in the F222M mosaic and measured the photometric offset between the PSF fitting and the aperture photometry. We used aper-

¹ Harvard Smithsonian Center for Astrophysics, MS-65, 60 Garden St, Cambridge, MA 02138 (tmegeath@cfa.harvard.edu)

² European Southern Observatory, K-Schwarzschild-Str. 2, 85748 Garching, Germany

³ On leave from the Max Planck Institut für Radioastronomie, 69 Auf dem Hügel, Bonn, 53121 Bonn, Germany

⁴ Department of Physics and Astronomy, Arizona State University, Tempe AZ 85287

ture photometry for the remaining point sources in the F222M and F160W mosaics, including the more isolated NIR3 and NIR5 sources. The total count rates were measured over a 3 pixel aperture with a 5 to 10 pixel sky radius. To determine magnitudes we used the equation $m = -2.5 \times \log(\text{PHOTFNU} \times \text{CR}/F_\nu(\text{Vega})) + \text{Corr}$, where CR is the count rate in (DN/sec), $\text{PHOTFNU} = 2.077 \times 10^{-6}$ and 5.502×10^{-6} , $F_\nu(\text{Vega}) = 1040.7$ and 610.4, and *Corr* - the aperture correction - is -0.53 and -0.71 for the F160W and F222M bands, respectively. The coefficients are the Cycle 7 values taken from the online NICMOS data handbook, the aperture corrections were measured from the data. The resulting zero points for the count rate were 19.40 and 21.22 for the F222M and F160W bands.

3. RESULTS

In the center of the W3 IRS 5 cluster is a small group of red objects, the most prominent of which is the double near-IR source IRS 5 (Figures 1 and 2). In Figure 1, we use lower limits to the colors of sources undetected at F160W by adopting the 10σ detection limit of 20.56 mag. Within a region less than $3''$ in diameter, there are three sources with $[F160] - [F222] > 4$, and two additional sources which have colors $[F160] - [F222] > 2$. We designate these sources NIR 1 – 5. The five sources are coincident with a dense clump of molecular gas, with a mass of $100 M_\odot$ and FWHM diameter of $5''$ or $9000 AU$ (Tieftrunk et al. 1995; 1997, Roberts, Crutcher, & Troland 1997). Tieftrunk et al. (1995) measure a column density of $5.8 \times 10^{23} \text{ cm}^{-2}$ toward this region with an $11''$ beam; the extinction through this clump in the F222M band is 60 magnitudes (Draine 1989). Consequently, we find it highly unlikely that the detected stars are background stars.

Images of the W3 IRS 5 system in the F160W and F222M filter are shown in Figure 3. Wilson et al. (2003) found that the two brightest infrared sources, NIR1 and NIR2, are coincident with hypercompact HII regions *D2* and *B*. These were detected in the mid-IR by van der Tak, Dianchi, & Tuthill (2005). NIR3 was also detected in the radio continuum and mid-IR by van der Tak, Dianchi, & Tuthill (2005). To the east, there are two additional sources, NIR4 and NIR5, which were not detected in the radio or mid-IR. In panel C, we show the same image with the two hypercompact HII regions subtracted using a PSF generated with Tiny Tim (Krist & Hook 1997). The subtracted image reveals two point sources near source NIR2; these are separated from NIR2 by $0.3''$ and $0.4''$. We designate these sources NIR2a and NIR2b. In between NIR1 and NIR2 we find an elongated nebulosity.

In Table 1 we give the properties of the seven unresolved sources in this region. The coordinates were shifted so that NIR1 has the same position as the *D2* source in Wilson et al. (2003). Only two sources were marginally detected in the F160M band, NIR1 and NIR4. The measured magnitudes for NIR1 and NIR2 are 21.386 and 21.392, both having 4.5σ detections.

The detection of NIR1, NIR2 and NIR3 at radio and mid-IR wavelengths essentially confirms that these are young OB stars embedded in the molecular core. NIR4 does not have a detected HII region, suggesting that either the emission is quenched by a high accretion rate

TABLE 1
NEAR-IR SOURCES

	R.A. (J2000)	Dec (J2000)	F222M Mag (unc)	Sep. ¹ A.U.	P.A. ¹ Deg.	Associated Radio or Mid-IR Source
1	2 25 40.784	62 05 52.62	12.21 (.03)	2252	37	D2 ² /Q5 ³ /K7 ³ /MIR1 ³
2	2 25 40.680	62 05 51.63	13.40 (.03)	-	-	B ² /Q3 ³ /K4 ³ /MIR2 ³
2a	2 25 40.690	62 05 51.91	14.78 (.07)	519	14	-
2b	2 25 40.682	62 05 51.23	16.38 (.07)	730	177	-
3	2 25 40.727	62 05 49.93	17.94 (.10)	3176	169	Q4 ³ /K6 ³ /MIR3 ³
4	2 25 40.896	62 05 51.71	16.20 (.07)	2780	87	-
5	2 25 41.040	62 05 52.10	17.94 (.10)	4712	80	-

¹Separation (Sep.) and Position Angle (P.A.) measured relative to NIR2. Separations assume a distance of 1830 pc (Imai et al. 2000)

²Associated 2 cm radio source using nomenclature of Claussen et al. (1994), also detected at 1.3 and 0.7 cm by Wilson et al. (2003)

³Associated 1.3 cm, 0.7 cm or mid-IR source using nomenclature of van der Tak, Dianchi, & Tuthill (2005)

(Keto 2003), that the star is not hot enough to produce significant Lyman continuum radiation, or that NIR4 is a background star - which is unlikely given the high extinction. Using the tentative F160W detection, NIR4 has a color of $(F160W - F222M) = 5.2$. Assuming that the emission from NIR4 is from a hot photosphere with no contribution from circumstellar dust, implying an intrinsic color of $(F160W - F222M) = 0$, and adopting a reddening law of $A_\lambda/E(J - H) = 2.4 \times \lambda^{(-1.75)}$ (Draine 1989) and a distance modulus of 11.23, we derive an absolute F222M magnitude of $M_{222} = -1.7$. Using the tabulation of *K*-band magnitudes vs mass for ZAMS OB stars in Hanson, Howarth, & Conti (1997), this magnitude corresponds to a spectral type B0.5V and a mass of $11 M_\odot$. The lack of radio emission suggests that the star has a later spectral type than B0.5, and it is likely that NIR4 is a later type star undergoing pre-main sequence evolution. For example, the Herbig Ae/Be star BD+65 1637, which has a spectral type of B3 and a mass of $9.5 M_\odot$, has a dereddened absolute *K*-band magnitude of -1.5 , similar to the of NIR4 (Hillenbrand, Strom, Vrba & Keene 1992). The Lyman continuum flux of a B3 star is 3% that of a B1 star (Panagia 1973). For NIR5 there is only a lower limit to the measured color, $(F160W - F222M) > 2.7$. Assuming an intrinsic color of $(F160W - F222M) = 0.025$ (i.e. equal to the *H* - *K* color with an M3 dwarf Bessell & Brett (1988)), the resulting absolute magnitudes in the F222M band is < 3.2 , corresponding to masses > 0.13 and $> 0.3 M_\odot$ for ages of 0.1 Myr and 1 Myr respectively (Muench et al. 2002). This source is probably a low mass star.

The two remaining point sources are found within a projected distance of 800 AU of NIR2; given their proximity to NIR2 and their red colors, we find it likely that these are stellar companions to NIR2. Neither of these sources would be resolved in the mid-IR imaging of van der Tak, Dianchi, & Tuthill (2005), but they would be resolved in VLA radio observations of this region. We see no radio counterpart to the fainter source, NIR2b, this source has the same magnitude as NIR5 and is prob-

ably a low mass star. NIR2a is directly between the radio sources *B* and *A*. If the $2.22\ \mu\text{m}$ emission from NIR2a is pure photospheric emission from an embedded star, the star would have to be quite massive; the upper limit of the dereddened F222M magnitude is equivalent to that of a ZAMS O8.5 star (Hanson, Howarth, & Conti 1997). An alternative explanation is that the two sources are unresolved knots of shocked H_2 from a bipolar flow originating from NIR2. Wilson et al. (2003) argued that NIR2/radio source *B* was driving an outflow in a roughly north-south direction; as shown in Figure 3, the two features are relatively aligned with the flow. These two explanations can be tested through narrow-band images in the $\text{H}_2\ 1 \rightarrow 0\ \text{S}(1)$ line.

We also report the first detection of a compact nebula between the NIR1 and NIR2. The nebula may result from the collision of outflows from NIR1 and NIR2, or from the collision of an outflow of one source with the envelope of the other. Wilson et al. (2003) and van der Tak, Dianchi, & Tuthill (2005) find evidence for a ionized knot moving from NIR1 at $100\ \text{km s}^{-1}$ which may be part of an outflow moving to the north-east. If the proposed outflow is bipolar and centered on NIR1, the counter-flow would be moving to the south-west in the direction of NIR2. Observations of Claussen et al. (1994) showed a radio source between NIR1 and NIR2, *D1*, which was not detected in subsequent VLA imaging. Wilson et al. (2003) argue that these transient radio sources are created in outflows, in this case *D1* may tracing the outflow responsible for the observed near-IR nebula. We speculate that the X-rays detected by Hofner et al. (2002) toward W3 IRS5 may originate in this nebula.

3.1. Discussion

Could W3 IRS 5 be a precursor to a Trapezium still embedded in its natal gas? Trapezia are defined as non-hierarchical multiple system of three or more stars; Abt & Corbally (2000) proposed that as a working rule for identifying Trapezia, the largest projected separation should be no more than three times the smallest projected separation. The separations between the five near-IR sources ranges between 5600 AU and 1800 AU and roughly satisfy this criteria. At smaller separations, the detection of candidate companions around NIR2 pro-

vides the first evidence for multiplicity at separations < 1000 AU around high-mass protostars. Companions with separations ranging from 460 AU to 16 AU have been detected toward the OB stars composing the Orion Nebula Trapezium system (Weigelt 1999). Hence, the spatial distribution of the primaries, and the presence of companions is similar to that observed in other Trapezium system.

The maximum projected separation of the five near-IR sources is 5600 AU, compared to 10000 AU for the Trapezium in the Orion Nebula. Abt & Corbally (2000) identified fourteen likely Trapezia, the median radius to the furthest outlying member of these Trapezia is 40000 AU. Hence, the projected separations in the W3 IRS 5 system are smaller than those observed in optically visible Trapezia. The stellar surface density of the five near-IR sources composing the W3 IRS 5 Trapezia is $10000\ \text{pc}^{-2}$, four times the density in the surrounding cluster - which is $2600\ \text{pc}^{-2}$ for a cluster radius of $21''$ (Megeath et al. 1996).

The small size of the W3 IRS 5 system may be a function of its youth; such systems may expand as the natal gas is expelled from the system by outflows and radiation. Maps of the molecular gas show a compact core of dense gas surrounding the W3 IRS 5 with a mass of $\sim 100\ M_{\odot}$ (Tieftrunk et al. 1995, Tieftrunk, Gaume & Wilson 1998, Roberts, Crutcher, & Troland 1997). The Lyman-continuum fluxes required by the observed radio continuum fluxes imply spectral types of B0.5 for the stars associated with NIR1, NIR2 and NIR4 (Wilson et al. 2003, van der Tak, Dianchi, & Tuthill 2005, Vacca, Garmany & Shull 1996). Since the radio continuum measurements suffer from a high optical depth, this is a lower limit. A B0.5 star has a mass around $18\ M_{\odot}$ (Vacca, Garmany & Shull 1996), this gives a lower limit to the combined stellar mass of $54\ M_{\odot}$. Megeath et al. (1996) found that the star formation efficiency, i.e. the ratio to the stellar mass to the total stellar and gas mass is about 18% in the W3 IRS 5 cluster. However, in the IRS 5 system, the stellar mass appears to be $> 30\%$ of the total mass. This high star formation efficiency may allow Trapezia to survive the dispersal of the natal gas and emerge as bound systems within a larger cluster.

REFERENCES

- Ambartsumian, V. A. 1954, *Contrib. Byurakan Obs.*, 15, 3
 Abt, H. A., Corbally, C. J. 2000 *ApJ*, 541, 841.
 Bessell, M. S. & Brett, J. M. 1988, *PASP* 100, 1134.
 Bonnell, I. A., & Matthew, R. B. 2002 *MNRAS*, 336, 659
 Bonnell, I. A. & Davies, M. B. 1998 *MNRAS*295, 691
 Campbell, M. F., Butner, H. M., Harvey, P. M., Evans, N. J. II, Campbell, M. B., & Sarbey, C. N. 1995, *ApJ*, 454, 831
 Claussen, M. J., Gaume, R. A., Johnston, K. J. & Wilson, T. L. 1994, *ApJ*, 424, L41
 Draine, B. T. 1989, in *Proc. 22nd ESLAB Symp. on Infrared Spectroscopy in Astronomy*, ed. B. H. Kaldeich (ESA SP-290; Noordwijk ESA), 93
 Hanson, M. M., Howarth, I. D., & Conti, P. S. 1997, *ApJ*, 489, 698
 Hillenbrand, L. A., Strom, S. E., Vrba, F. J. & Keene, J. 1992, *ApJ*, 397, 613
 Hodapp, K.-W. 1994, *ApJS*, 94, 615
 Hofner, P., Delgado, H., Whitney, B., Churchwell, E., & Linz, H. 2002, *ApJ*, 579, L95
 Howell, R. R., McCarthy, D. W. & Low, F. J. 1981, *ApJ*, 251, L21
 Imai, H., Kameya, O., Sasao, T., Miyoshi, M., Deguchi, S., Horiuchi, S. & Asaki, Y. 2000, *ApJ*, 538, 751
 Keto, E. 2003, *ApJ*, 599, 1196
 Krist, J. E. & Hook, R. N. 1997, in *Proc. 1997 HST Calibration Workshop: With a New Generation of Instruments*, ed. S. Casertano et al. (Baltimore: STScI), 192
 Kroupa, P., Aarseth, S. & Hurley, J. 2001, *MNRAS*, 321, 669
 Megeath, S. T., Herter, T., Beichman, C., Gautier, N., Hester, J. J., Rayner, J. & Shupe, D. 1996, *A&A*, 307, 775
 Mermilliod, J.-C., & Garcia, B. 2001, in *IAU Symposium Vol 200, The Formation of Binary Stars*, eds. H. Zinnecker & R. D. Mathieu, 191
 Muench, A. A., Lada, E. A., Lada, C. J., & Alves, J. 2002, *ApJ*, 573, 366
 Neugebauer, G.; Becklin, E. E.; Matthews, K. 1982, *AJ*, 87, 395
 Panagia, N. 1973, *AJ*, 78, 929
 Roberts, D. A, Crutcher, R. M. & Troland, T. H. 1997, *ApJ*, 479, 318
 Sharpless, S. 1954, *ApJ*, 119, 334
 Sollins, P. & Megeath, S. T. 2004, *AJ*, 128, 2374

- Thompson, R.I., Rieke, M., Schneider, G., Hines, D.C. & Corbin, M.R. 1998, ApJ, 429, L95”
- Tieftrunk, A. R., Gaume, R. A. & Wilson, T. L. 1998, A&A, 340, 242
- Tieftrunk, A. R., Gaume, R. A., Claussen, M. J., Wilson, T. L. & Johnston, K. J. 1997, A&A, 318, 931
- Tieftrunk, A. R., Wilson, T. L., Steppe, H., Gaume, R. A., Johnston, K. J. & Claussen, M. J. 1995, A&A, 303, 901
- Vacca, W. D., Garmany, C. D. & Shull, J. M. 1996, ApJ, 460, 914
- van der Tak, F. F. S., Tuthill, P. G., & Danchi, W. C., 2005, A&A, in press
- Wainscoat, R. J., Cohen, M., Volk, K., Walker, H. J. & Schwartz, D. E. 1992, ApJS, 83, 111
- Weigelt, G., Balega, Y., Preibisch, T., Shehertl, D., Schöler, M. & Zinnecker, H. 1999, A&A, 347, L15
- Wilson, T.L., Boboltz, D. A., Gaume, R. A., & Megeath, S. T. ApJ, 597, 434

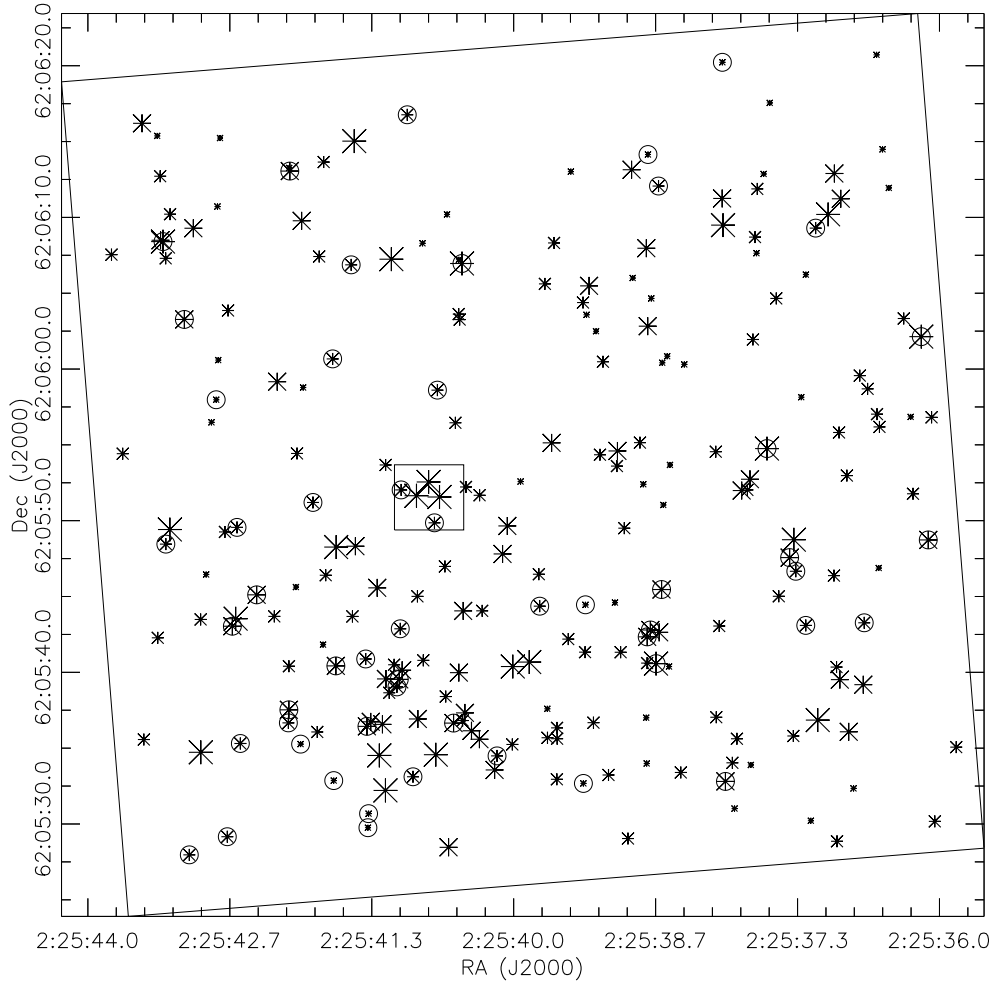


FIG. 1.— The distribution of red sources detected in the F222M band. The size of the asterisk depends on the color of the source, ranging from $1 < (F160W - F222M) \leq 2$ for the smallest asterisks, $2 < (F160W - F222M) \leq 3$, $3 < (F160W - F222M) \leq 4$ and $(F160W - F222M) > 4$ for the largest asterisks. For sources undetected in the F160W band, a magnitude of 20.56, equivalent to a 10σ detection, is given as a lower limit. Sources with only lower limits to their colors are marked by circles; their colors may be redder than indicated by the size of the asterisk. The outer box shows the extent of the field imaged with NICMOS, the inner square is the region displayed in Figure 3.

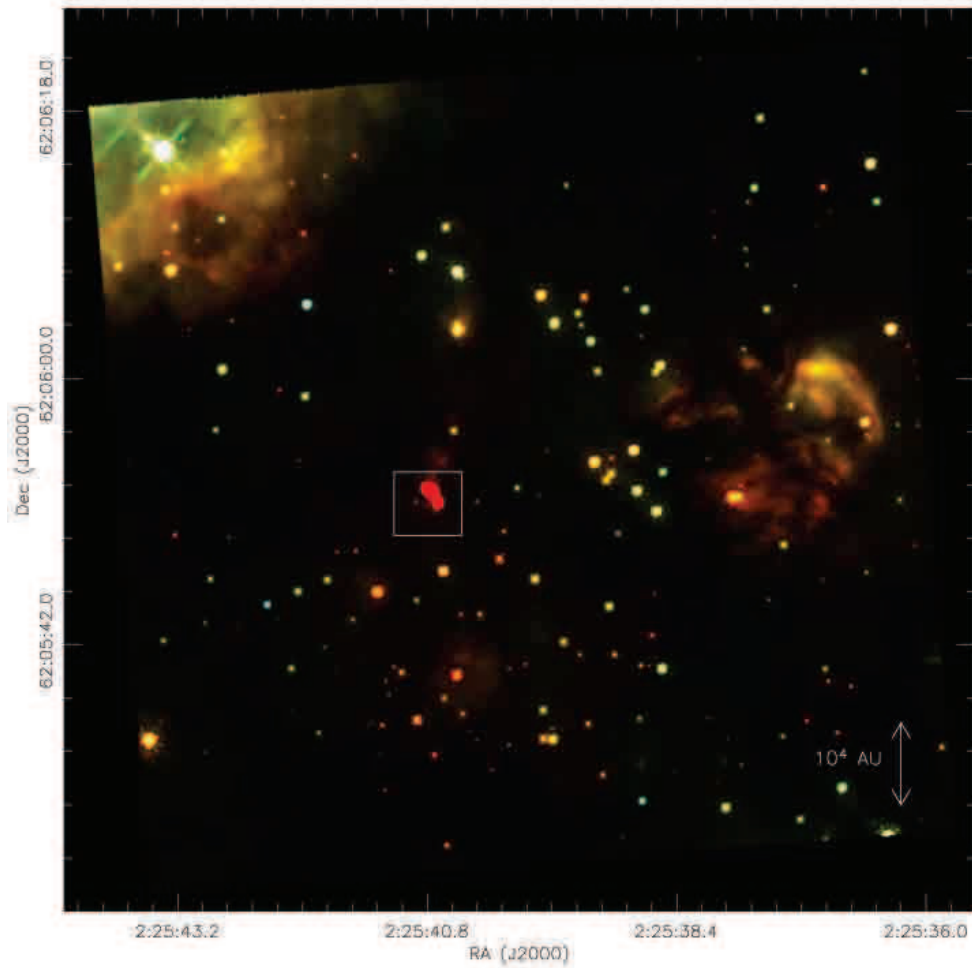


FIG. 2.— A color composite image constructed from the F110W (blue), F160W (green) and F222M (red) mosaics of the W3 IRS 5 region, encompassing the whole region surveyed in the NICMOS measurements. The box shows the region displayed in Figure 3.

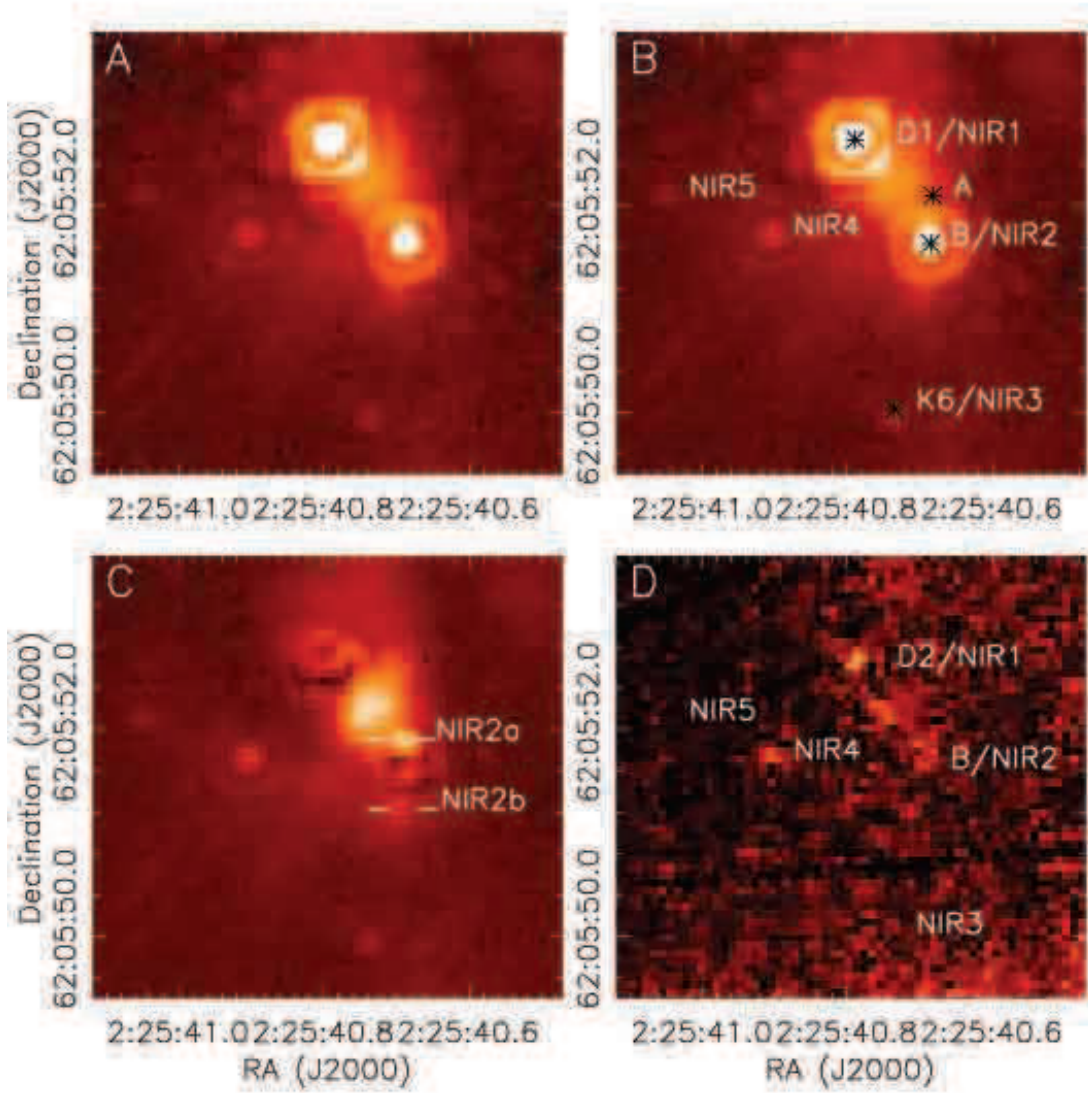


FIG. 3.— F222M (2.22 μm) and F160W (1.60 μm) images of W3 IRS 5 and the neighboring red sources and nebulosities. In Panel A we show the F222M image using a cube root scaling. In Panel B we show the same image, with the main NIR sources marked. The asterisks mark the positions of the associated radio sources *D2*, *B*, *A* and *K6*. In Panel C we show the image with the NIR1 and NIR2 sources subtracted. An extended nebulosity between the two sources is clearly evident. Two additional point sources partially hidden by the PSF of NIR2 are marked. The ring-like pattern is a residual from the PSF subtraction. In Panel D we show the F160W image toward this region, with the five IR sources marked.